Yaw Stability Control of an Automotive Vehicle via Generalized Predictive Algorithm

Sohel Anwar

Abstract—**Yaw stability of an automotive vehicle in a steering maneuver is critical to the overall safety of the vehicle. In this paper we present a theoretical development and experimental results of a vehicle yaw stability control system based on generalized predictive control (GPC) method. The controller tries to predict the future yaw rate of the vehicle and then takes control action at present time based on future yaw rate error. The proposed controller utilizes the insight into the yaw rate error growth when the automobile is in an understeer or oversteer condition on a low friction coefficient surface in a handling maneuver. Experimental results show that the predictive feature of the proposed controller provides an effective way to control the yaw stability of a vehicle.**

I. INTRODUCTION

YAW Stability Control (YSC) systems have been established in the automotive industry as a safety/performance feature. YSC generally prevents the vehicle from under-steering or over-steering in a handling maneuver (e.g. lane change, slalom, etc.), particularly on a low friction coefficient surface. It also helps the driver maintain yaw stability of the vehicle in a high G handling maneuver.

A predictive yaw stability controller based on GPC [1] is presented in this paper. The predictive nature of the control algorithm would provide an insight into the incipient yaw instability that can be controlled with appropriate actuation system. This feature may improve the performance of the vehicle yaw stability (i.e. response, etc.), particularly on low friction coefficient surfaces. The control algorithm compares the vehicle yaw rate from a production grade yaw rate sensor with a desired value (which is computed based on vehicle speed and steering wheel angle). If the yaw rate error (the difference between the desired and measured yaw rate) exceeds a certain threshold, a controlling yaw moment is calculated based on a predictive control strategy. This yaw torque command is then translated into actuator command(s).

Manuscript received September 14, 2004. This work was supported by the Chassis Advanced Technology Department of Visteon Corporation.

S. Anwar was with the Chassis Advanced Technology Department, Visteon Corporation, Dearborn, MI 48126 USA. He is currently with the Mechanical Engineering Department, Purdue School of Engineering and Technology, IUPUI, Indianapolis, IN 46202 USA (phone: 317-274-7640; fax: 317-274-9744; e-mail: soanwar@ iupui.edu).

Sato et al [2] investigated a four wheel steering system with the use of yaw rate feedback and steering angle feedforward control. When the vehicle deflects due to a sudden side wind, road surface disturbance, or abrupt braking, steering is automatically corrected through the rear wheel to significantly improve forward stability. Shibahata et al [3] discussed a chassis control strategy for improving the limit performance of vehicle motion. They studied the effects of braking force distribution on a vehicle's lateral and longitudinal directions. It was claimed that controlling the lateral distribution of the braking force on the front wheels was effective for the improvement of the vehicle stability while that on the rear wheels was effective for extending the limit of vehicle motion. Wang et al [4] presented a method to improve the handling and stability of vehicles by controlling yaw moment generated by driving / braking forces. Yaw moment was controlled by the feedforward compensation of steering angle and velocity to minimize the side slip angle at the vehicle center of gravity. They provided simulation results and scaled experimental results to verify their claims. Wang and Nagai [5] discussed an integrated control system providing high performance within tires' strong nonlinear areas with adaptability to the changing road and other conditions, by optimally controlling the front and rear steering angles and the yaw moment, based on the information of system parameters. Simulation results were provided to prove the claims. Savkoor and Chou [6] investigated the application of active aerodynamic devices for suppressing parasitic motion and for improving the response of vehicles to steering maneuvers, within the scope of the linear dynamic behavior. The improvements in the performance of the base-line vehicle that were achievable by the application of direct yaw and roll moments by applying either an open loop control pre-filter or a state feedback control law based on LQR design. They observed that the control strategy yielded a superior performance but demanded unreasonably large moments from the actuators in the context of available aerodynamic forces. They also observed that the demand on direct yaw and roll moment of actuators is modest when the actuators are controlled using the LQR feedback only and if the control design was used to track a desired yaw rate trajectory and simultaneously to reduce the parasitic rolling motion. Nagai et al [7] presented an integrated control system of active rear wheel steering and yaw moment

control using braking forces. Considering the tire friction circle, the control system was designed using model matching control theory to make the vehicle performance follow a desired dynamics model even during large decelerations or lateral accelerations. They provided simulation results to verify the claims made. Park and Ahn [8] described an H-infinity yaw moment control scheme using brake torque for improving vehicle performance and stability specially in high speed driving. The controller was designed to minimize the difference between the performance of the actual vehicle behavior and that of its model behavior under disturbance input. An eight DOF vehicle model was used to verify the enhancement claims on vehicle performance and stability. Drakunov et al [9] investigated the application of sliding mode control on the yaw stability control for an automobile. The control law was based on optimum search for minimum yaw rate via sliding mode control. The developed algorithm determined the level of vehicle stability through the used of measured vehicle states and then intervened if necessary through individual wheel braking to provide added stability and handling predictability. Hac and Bodie [10] discussed a method of improving vehicle stability and emergency handling using electronically control chassis systems. They analyzed a simple nonlinear vehicle model in the yaw plane to show that the vehicles can become unstable during portions of handling maneuvers performed at or close to the limit of adhesion. They also showed that small changes in the balance of tire forces between front and rear axles may affect vehicle yaw moment and stability. They presented preliminary test results for a vehicle with integrated closed loop control of brakes and suspension, performing typical handling maneuvers.

The present work utilizes the predictive characteristics of the GPC to derive a yaw stability control algorithm. The control algorithm is based on a linearized vehicle model. This model is then discretized via a bilinear transformation. The control algorithm has been validated on a test vehicle. Experimental results show that the predictive controller is effective in minimizing the understeer and oversteer conditions.

II. LINEARIZED VEHICLE MODEL

Yaw Stability Control (YSC) System has been around on the high-end cars for a number of years. The effectiveness of these systems varies widely depending on the system design, road conditions and driver's response. Most of these systems are based on empirical data and heavily dependent on testing. In the present investigation, a more systematic approach is taken to develop an YSC system based on a linearized vehicle model and a predictive control algorithm. Figure 1 illustrates the forces acting on the tire contact patches for a vehicle during a handling maneuver. The yaw dynamics for the vehicle in such a maneuver can be described with following equation [12]:

$$I_{zz}\frac{dr}{dt} = a(F_{yFL}+F_{yFR})\cos\delta + b(F_{yRR}+F_{yRL}) + cF_{yFL}\sin\delta - dF_{yFR}\sin\delta + M_z \quad (1)$$

Where, I_{ZZ} = Vehicle yaw inertia; M_z = Control yaw moment; F_{xFL} , F_{yFL} , F_{xFR} , F_{yFR} , F_{xRL} , F_{yRR}, F_{yRR} = Tire contact patch forces in x- and y-directions as illustrated in Figure 1; δ = Road wheel angle for the front wheels; a, b, c, d = Contact patch locations from the vehicle C.G.;

For simplification, it was assumed in equation (1) that: (a) Road wheel angle for the front left tire is equal to the road wheel angle for the front right tire, and (b) The force in x-direction is very small in a non-braking situation.

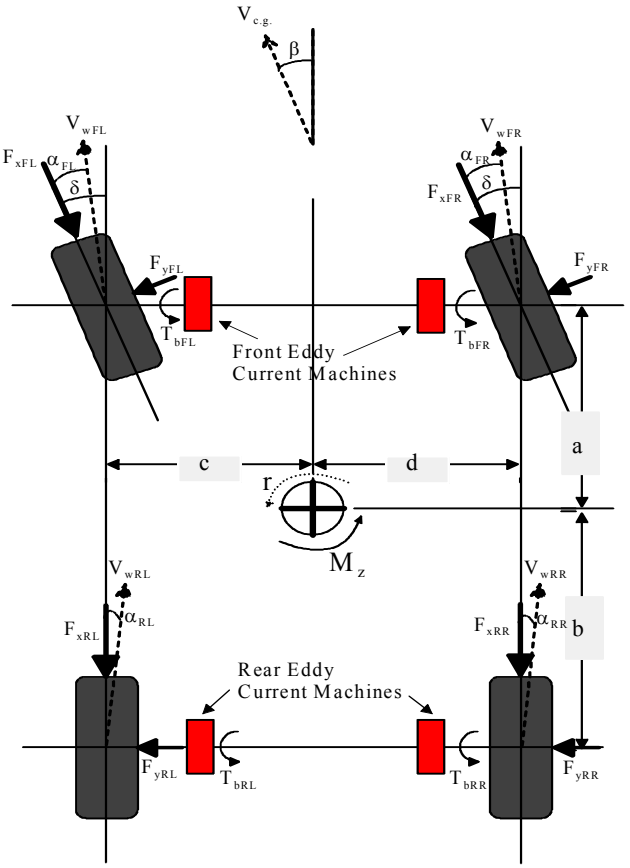

Figure 1 Schematic representing vehicle yaw dynamics.

It is further assumed that the normal force on the left and right side of the vehicle is same, i.e. normal force on the front left contact patch is the same as that on front right contact patch, etc.. However, the friction coefficient is assumed to the different for each contact patch. Also, the lateral friction forces are assumed to linearly vary with the slip angle [12].

$$\alpha_{FL} = \alpha_{FR} = \alpha_F; \alpha_{RL} = \alpha_{RR} = \alpha_R$$
$$F_{yFL} = c_{FL}\alpha_F; F_{yFR} = c_{FR}\alpha_F; F_{yRL} = c_{RL}\alpha_R; \quad (2)$$
$$F_{yRR} = c_{RR}\alpha_R$$

where c_{FL}, c_{FR}, c_{RL}, & c_{RR} are the cornering coefficients from a two track vehicle model. α_{FL}, α_{FR}, α_{RL},

& α_{RR} are slip angles associated with each wheel. μ_{FL}, μ_{FR}, μ_{RL}, & μ_{RR} are the friction coefficients associated with each road-tire contact patch.

With above simplification, the following yaw dynamics equation is obtained:

$$\dot{r} = \frac{1}{I_{zz}}\begin{bmatrix} a(c_{FL}+c_{FR})\alpha_F \cos\delta + b(c_{RL}+c_{RR})\alpha_R + \\ (c*c_{FL} - d*c_{FR})\alpha_F \sin\delta + M_z \end{bmatrix} \quad (3)$$

Now, the slip angles can be related to the body side slip angle, road wheel angle, and the yaw angle by the following relationship (figure 1).

$$\alpha_F = (\delta - \beta - \frac{r}{V_{cg}}a); \alpha_R = (-\beta + \frac{r}{V_{cg}}b) \quad (4)$$

Substituting the above relationship (4) in equation (3), and assuming the $c_{FL} = c_{FR} = c_F$ and $c_{RL} = c_{RR} = c_R$, the following equation is obtained:

$$\dot{r} = \frac{1}{I_{zz}}\begin{bmatrix} \{2ac_F \cos\delta + (c-d)c_F \sin\delta\}\delta - \{ \\ \{2ac_F \cos\delta + (c-d)c_F \sin\delta\}\frac{a}{V_{cg}} - \frac{2b^2 c_R}{V_{cg}}\}r - \\ \{2ac_F \cos\delta + (c-d)c_F \sin\delta + 2bc_R\}\beta + M_z \end{bmatrix} \quad (5)$$

Now, the side-slip and state equation is obtained as follows [12].

$$V_{cg}(\dot{\beta} + r) = \frac{1}{m_{cg}}\begin{bmatrix} (F_{xFL} + F_{xFR})\sin\delta - (F_{yFL} \\ + F_{yFR})\cos\delta - (F_{yRL} + F_{yRR}) \end{bmatrix}\cos\beta + \frac{1}{m_{cg}}\begin{bmatrix} (F_{xFL} + F_{xFR})\cos\delta + (F_{yFL} + F_{yFR})\sin\delta + \\ (F_{xRL} + F_{xRR}) \end{bmatrix}\sin\beta \quad (6)$$

Again, assuming that the forces in x-direction in a non-braking situation are very small, and substituting the relationship between slip angle & lateral forces, and the slip angle equation & assuming that variation of β is very small about the operating value, and using the assumption that $C_{FL} = C_{FR} = C_F$ and $C_{RL} = C_{RR} = C_R$, we obtain:

$$\dot{\beta} = -\frac{1}{V_{cg}m_{cg}}\begin{bmatrix} 2C_F(\delta - \beta)\cos\delta - 2C_R\beta - \\ 2C_F\frac{r}{V_{cg}}a\cos\delta + 2C_R\frac{r}{V_{cg}}b \end{bmatrix} - r \quad (7)$$

Combining the equations (5) and (7), we obtain:

$$\begin{bmatrix}\dot{\beta}\\ \dot{r}\end{bmatrix} = \begin{bmatrix} -\frac{2C_F\cos\delta + 2C_R}{V_{cg}m_{cg}} & -\frac{2aC_F\cos\delta - 2bC_R}{V_{cg}^2 m_{cg}} - 1 \\ \{2ac_F\cos\delta + (c-d)* & \{\{2ac_F\cos\delta + (c-d)* \\ -\frac{c_F\sin\delta - 2bc_R\}}{I_{zz}} & -\frac{c_F\sin\delta\}a - 2b^2 c_R\}}{V_{cg}I_{zz}} \end{bmatrix}\begin{bmatrix}\beta\\ r\end{bmatrix} + \begin{bmatrix} \frac{2C_F\cos\delta}{V_{cg}m_{cg}} \\ \frac{2ac_F\cos\delta + (c-d)c_F\sin\delta}{I_{zz}} \end{bmatrix}\delta + \begin{bmatrix}0\\ \frac{1}{I_{zz}}\end{bmatrix}M_z \quad (8)$$

Now for the sake of simplicity, let us linearize the above equation about δ = 0. The following equation of obtained:

$$\begin{bmatrix}\dot{\beta}\\ \dot{r}\end{bmatrix} = \begin{bmatrix} -\frac{2(C_F + C_R)}{V_{cg}m_{cg}} & -\frac{2(aC_F - bC_R)}{V_{cg}^2 m_{cg}} - 1 \\ -\frac{2(ac_F - 2bc_R)}{I_{zz}} & -\frac{2(a^2 c_F - b^2 c_R)}{V_{cg}I_{zz}} \end{bmatrix}\begin{bmatrix}\beta\\ r\end{bmatrix} + \begin{bmatrix}0\\ \frac{1}{I_{zz}}\end{bmatrix}M_z \quad (9)$$

Therefore the plant dynamics (vehicle yaw dynamics) can be represented by the following set of equations:

$$\begin{bmatrix}\dot{x}_1\\ \dot{x}_2\end{bmatrix} = \begin{bmatrix} a_{11} & a_{12} \\ a_{21} & a_{22}\end{bmatrix}\begin{bmatrix}x_1\\ x_2\end{bmatrix} + \begin{bmatrix}b_1\\ b_2\end{bmatrix}u; y = \begin{bmatrix}c_1 & c_2\end{bmatrix}\begin{bmatrix}x_1\\ x_2\end{bmatrix} \quad (10)$$

$$x_1 = \beta; x_2 = r; b_1 = 0; b_2 = \frac{1}{I_{zz}}; c_1 = 0; c_2 = 1$$

$$a_{11} = -\frac{2(C_F + C_R)}{V_{cg}m_{cg}}; a_{12} = -\frac{2(aC_F - bC_R)}{V_{cg}^2 m_{cg}} - 1$$

$$a_{21} = -\frac{2(ac_F - 2bc_R)}{I_{zz}}; a_{22} = -\frac{2(a^2 c_F - b^2 c_R)}{V_{cg}I_{zz}}$$

A transfer function representation of the above state-space system is given by the following equation:

$$\frac{R(s)}{M_z(s)} = \frac{(s - a_{11})/I_{zz}}{s^2 - (a_{11} + a_{22})s + (a_{11}a_{22} - a_{12}a_{21})} \quad (11)$$

The above transfer function can be discretized in order to obtain a discrete time transfer function. A bilinear transformation is utilized for this purpose.

$$\frac{R(z)}{M_z(z)} = \frac{(n_0 + n_1 z^{-1} + n_2 z^{-2})}{(d_0 + d_1 z^{-1} + d_2 z^{-2})}; n_0 = \frac{1}{I_{zz}}(2T - a_{11}T^2);$$

$$n_1 = -\frac{2a_{11}T^2}{I_{zz}}; n_2 = -\frac{1}{I_{zz}}(2T + a_{11}T^2)$$

$$d_0 = T^2(a_{11}a_{22} - a_{12}a_{21}) - 2T(a_{11} + a_{22}) + 4 \quad (12)$$

$$d_1 = 2T^2(a_{11}a_{22} - a_{12}a_{21}) - 8$$

$$d_2 = T^2(a_{11}a_{22} - a_{12}a_{21}) + 2T(a_{11} + a_{22}) + 4$$

In the above set of equations, T represents the sample time.

III. Predictive Control Law

Like most of the YSC algorithm, the proposed control algorithm also requires the knowledge of desired vehicle yaw rate, given the steering angle and vehicle speed. The objective of the controller is to track the desired yaw rate by minimizing the sum of future yaw rate errors.

$$J = \sum_{j=0}^{N}[r_{des}(t+j) - r(t+j)]^2 \quad (13)$$

J = Yaw rate performance index for the vehicle

N = Prediction horizon

$r_{des}(t+j)$ = Desired yaw rate at time (t+j)

$r(t+j)$ = Predicted yaw rate at time (t+j)

Generalized predictive control (GPC) utilizes Diophantine type discrete mathematical identities to obtain predicted plant output in the future. In addition to its predictive capabilities, GPC has been shown to be robust against modeling errors and external disturbances [1]. In the following section, a discrete version of the GPC (Generalized Predictive Control) is derived.

The transfer function in equation (13) can be rewritten as:

$$(d_0 + d_1 z^{-1} + d_2 z^{-2}) R(z) = (n_0 + n_1 z^{-1} + n_2 z^{-2}) M_z(z) \quad (14)$$

Now the Diophantine prediction equation (j-step ahead predictor) is given by,

$$E_j(z^{-1})(d_0 + d_1 z^{-1} + d_2 z^{-2})\Delta + z^{-j} F_j(z^{-1}) = 1 \quad (15)$$

$E_j(z^{-1})$ = A polynomial in z^{-1} with order (j-1)

$F_j(z^{-1})$ = A polynomial in z^{-1} of degree 1.

Multiplying both sides of equation (16) by $r(t+j)$,

$$r(t+j) = F_j r(t) + E_j(n_0 + n_1 z^{-1} + n_2 z^{-2})\Delta M_z(t+j-1) \quad (16)$$

The objective function can now be rewritten in matrix format as,

$$J = [R_{Des} - R]^T [R_{Des} - R] \quad (17)$$

$$R_{Des} = [r_{Des}(t+1) r_{Des}(t+2) ..... r_{Des}(t+N)]$$

$$R = [R(t+1) R(t+2) ..... R(t+N)]$$

$$R(t+1) = F_1 r(t) + G_1 \Delta M_z(t)$$

.

$$R(t+N) = F_N r(t) + G_N \Delta M_z(t+N-1)$$

$$G_j(z^{-1}) = E_j(z^{-1})(n_0 + n_1 z^{-1} + n_2 z^{-2})$$

The predicted slip equations can be re-written in a matrix format as follows:

$$R = G * U + f$$

$$G = \begin{bmatrix} g_0 & 0 & . & . & 0 \\ g_1 & g_0 & . & . & 0 \\ . & . & . & . & . \\ . & . & . & . & . \\ g_{N-1} & g_{N-2} & . & . & g_0 \end{bmatrix}$$

$$U = [\Delta M_z(t) \Delta M_z(t+1) .... \Delta M_z(t+N-1)]^T$$

$$f = [f(t+1) f(t+2) .... f(t+N)]^T \quad (18)$$

$$f(t+1) = [G_1(z^{-1}) - g_{10}]\Delta M_z(t) + F_1 r(t)$$

..

$$G_i(z^{-1}) = g_{i0} + g_{i1} z^{-1} + ...$$

The objective function can now be rewritten as follows:

$$J = [R_{Des} - f - GU]^T [R_{Des} - f - GU] \quad (19)$$

Minimization of the objective function yield the following predictive control law:

$$U = [G^T G]^{-1} G^T (R_{Des} - f) \quad (20)$$

In the above equation, U is a vector. To obtain the control law at present time, only the first element of U is used. Therefore the control law is given by:

$$\Delta M_z(t) = \Delta M_z(t-1) + g^T (R_{Des} - f) \quad (21)$$

where g^T is the first row of $[G^T G]^{-1} G^T$.

Equation (21) is the predictive control law for the yaw stability control system.

Now, the control moment can be generated via a number of actuation systems. In this particular research work we present an electromagnetic brake-by-wire based yaw control system. The yaw moment is generated by selectively energizing these EM brakes which are located at the four corners of the vehicle. Let's first develop the control law in terms of M_z then we will present the electromagnetic means to deliver the yaw moment. There are two situations that accompanies yaw instability: a) Understeer condition and b) Oversteer condition. In an understeer condition the absolute value of the vehicle yaw rate r is always smaller than the absolute value of desired vehicle yaw rate r_{des}. In an oversteer condition, the absolute value of the vehicle yaw rate r is always larger than the absolute value of desired vehicle yaw rate r_{des}. In an understeer condition, the control moment is generated by applying braking torque on the inner wheels whereas in an oversteer condition the control yaw moment is generated by applying braking torque on the outer wheels. Now the amount of braking torque on the wheels is dictated by the control yaw torque M_z. In any of these two vehicle dynamic conditions, either both wheels or one wheel (on one side) can be braked to generate M_z. In case of braking only one wheel, however, it has been observed that braking the front wheel is more effective in an oversteer condition whereas braking the rear wheel has been found to be more effective in an understeer condition. From an optimal control point of view, it is recommended to use only one wheel to generate the control moment.

Based on the above analysis, the control yaw moment can be related to brake torques as follows (applied braking forces act only in the direction of tire longitudinal axes).

Assuming counterclockwise positive,

$$M_z = cF_{xFL}\cos\delta - aF_{xFL}\sin\delta - dF_{xFR}\cos\delta - aF_{xFR}\sin\delta + cF_{RL} - dF_{RR} \quad (22)$$

Understeer Condition:

Vehicle turning counterclockwise: brake rear left wheel

$$M_z = cF_{xRL} = c\frac{T_{bRL}}{R}; T_{bRL} = \frac{R}{c}M_z \quad (23)$$

Vehicle turning clockwise: brake rear right wheel

$$M_z = dF_{xRR} = d\frac{T_{bRR}}{R}; T_{bRR} = \frac{R}{d}M_z \quad (24)$$

Oversteer Condition:

Vehicle turning counterclockwise: brake front right wheel

$$M_z = (d\cos\delta - a\sin\delta)\frac{T_{bFR}}{R}; T_{bFR} = \frac{R}{(d\cos\delta - a\sin\delta)}M_z \quad (25)$$

Vehicle turning clockwise: brake front left wheel

$$M_z = (c\cos\delta - a\sin\delta)\frac{T_{bFL}}{R}; T_{bFL} = \frac{R}{(c\cos\delta - a\sin\delta)}M_z \quad (26)$$

Since the electromagnetic brakes torque is a function of rotor speed, in certain situations these actuators may saturate. In case of actuator saturation, one wheel actuator may not be able to deliver the requested yaw moment. In this condition, both front and rear wheel actuators can be used to generate the requested yaw moment.

First we need a torque estimation algorithm for the eddy current machines. Reference [11] describes a torque estimation algorithm for an eddy current machine given the rotor speed and excitation current as follows:

$$T_{est} = f_0(\omega) + f_1(\omega) * i + f_2(\omega) * i^2 \qquad (27)$$

T = retarding torque; i = retarder feedback current

$$f_i(\omega) = a_{i0} + a_{i1}\omega + a_{i2}\omega^2 \qquad (28)$$

a_{i0} , a_{i1} , a_{i2} = identified parameters; ω = rotor speed

Equations (23) through (27) represent the control law for the yaw management system proposed in this paper. It is assumed that means of estimating the tire-road friction coefficient and normal force on the each tire is available. Also, the desired yaw rate is also assumed to be known a priori either via experimental data or data from previous developments.

IV. EXPERIMENTAL RESULTS

The above control law (23)-(27) has been implemented on test vehicle equipped with a hybrid electromagnetic-electro-hydraulic brake-by-wire system. Since these equations will provide yaw stability control functionality based on a predetermined desired yaw rate, it is necessary to have this data a priori. Also, for a smooth vehicle ride and handling it is desired to activate the yaw moment controller based on a threshold value for the yaw rate error. In the following experimental results, this yaw rate error threshold was set at 5 degrees per second.

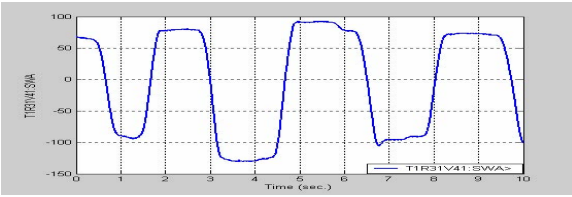

Figure 2 Steering wheel angle in a slalom maneuver on snow without yaw stability control.

A vehicle speed estimator, which is not the subject of this paper, is utilized to obtain the vehicle speed. Wheel speed is obtained for production grade wheel speed sensors.

Figures 2 through 5 show the braking experimental results for a slalom maneuver on packed snow without any yaw stability control. These figures show the baseline performance of the vehicle.

It is evident from figures 4 and 5 that the vehicle understeers heavily on the packed snow surface. The measured vehicle yaw rate significantly lags the desired yaw rate for the given steering angle and vehicle speed.

Now experimental results with the predictive yaw stability controller are presented. The following controller parameter values were determined experimentally which resulted in the optimal performance of the controller:

Prediction Horizon = 3; Control Horizon = 1; Speed

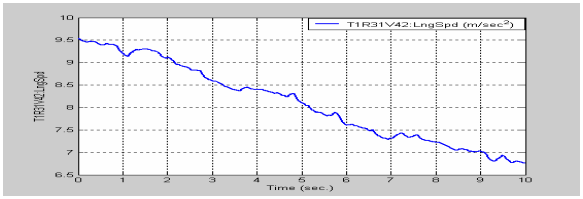

Figure 3 Vehicle speed in a slalom maneuver on snow without yaw stability control.

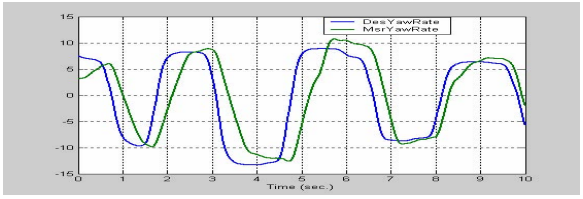

Figure 4 Desired and measured yaw rate in a slalom maneuver on snow without yaw stability control.

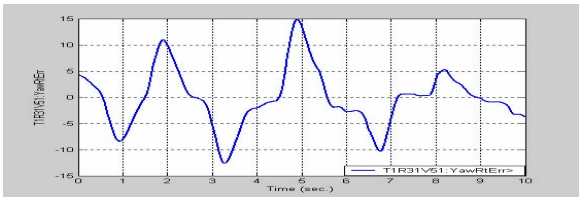

Figure 5 Yaw rate error in a slalom maneuver on snow without yaw stability control.

threshold for YTC activation = 4 kph; Yaw rate error threshold for YTC activation = +/- 5 degrees

Figures 6 and 7 show the steering wheel angle and vehicle speed for the test vehicle with stability control. The steering wheel input is similar to the previous case. However, the vehicle speed is a function of the vehicle yaw performance, since the driver tends to reduce the vehicle speed when the yaw rate error is large. Hence, the vehicle speed profile differs from the previous case.

The normal force on each wheel is estimated from the static weight distribution and dynamic weight transfer in an acceleration/deceleration event.

Figure 8 shows desired and measured vehicle yaw rates and the yaw rate error respectively in a slalom maneuver on a packed snow surface. It is clear that the yaw rate error is very small compare to the previous case. The vehicle yaw rate tracks the desired yaw rate fairly well and as a result the vehicle speed could be kept relatively higher throughout

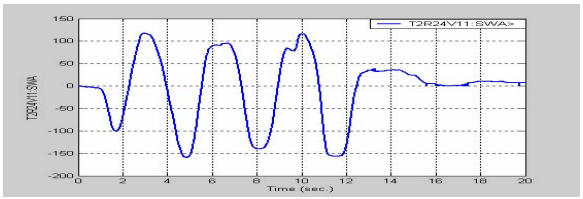

Figure 6 Steering wheel angle in a slalom maneuver on snow with yaw stability control.

the maneuver.

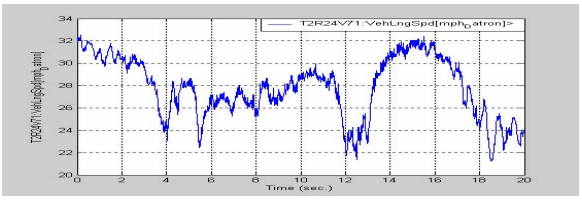

Figure 7 Vehicle speed in a slalom maneuver on snow with yaw stability control.

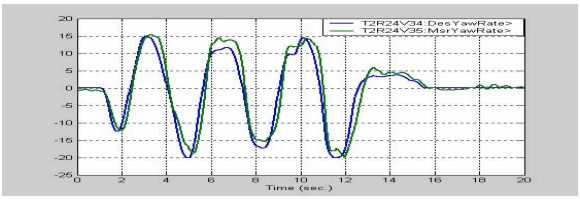

Figure 8 Desired and measured yaw rate in a slalom maneuver on snow with yaw stability control.

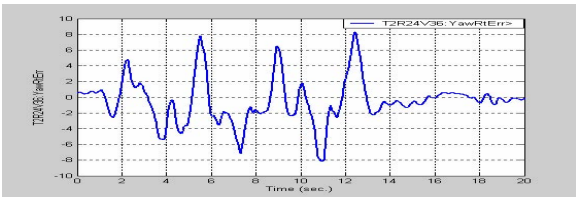

Figure 9 Yaw rate error in a slalom maneuver on snow with yaw stability control.

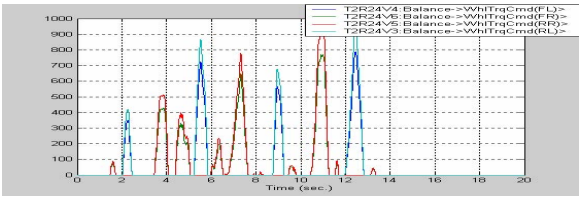

Figure 10 Wheel braking torque command in a slalom maneuver on snow with yaw stability control.

Figures 9 and 10 show the yaw rate error for the vehicle and the wheel braking torque command from the controller respectively.

V. CONCLUSIONS

A generalized predictive control law has been derived for a simplified linear vehicle model for a brake based yaw stability control system. The predictive nature of the controller has been utilized to predict the yaw rate error growth which is then utilized to derive the control law. Experimental results show that the vehicle can be effectively stabilized in an oversteer/understeer condition on a packed snow surface using the predictive controller. The vehicle speed could be kept at relatively higher value throughout the slalom maneuver. The measured yaw rate has been found to track the desired yaw rate well.

REFERENCES

[1] Clarke, D.W, Mohtadi, C., Tuffs, P.S., "Generalized Predictive Control – Part I. The Basic Algorithm", *Automatica*, Vol. 23, No. 2, pp. 137-148, 1987.

[2] Sato, H., Kawai, H., and Hitisikoike, M., "Development for four wheel steering system using yaw rte feedback control", 1991, *SAE technical paper series – Passenger Car Meeting and Exposition*, September 16-19, 1991, Nashville, TN, USA.

[3] Shibahata, Y., Shimada, A.M., Shimada, K., Furukawa, Y., "Improvement on limit performance of vehicle motion by chassis control", *Vehicle System Dynamics*, v 23, n SUPPL, 1994.

[4] Wang, Y., Morimoto, T., and Nagai, M., "Motion Control of front-wheel-steering vehicles by yaw moment compensation (Comparison with 4WS Performance)", *Transactions of the Japan Society of Mechanical Engineers,* Part C, v 60, n571, Mar, 1994, pp.912-917.

[5] Wang, Y. and Nagai, M., "Integrated control of four-wheel-steer and yaw moment to improve dynamic stability margin", *Proceedings of the IEEE Conference on Decision and Control*, v 2, December 11-13, 1996, Kobe, Japan, pp 1783-1784.

[6] Savkoor, A.R. and Chou, C.T., "Application of aerodynamic actuators to improve vehicle handling", *Vehicle System Dynamics*, v32, n4, 1999, pp.345- 374.

[7] Nagai, M., Yamanaka, S., and Hirano, Y., "Integrated control of active rear wheel steering and yaw moment control using braking forces", *JSME International Journal,* Series C, v 42, n 2, 1999, pp 301-308.

[8] Park, J.H. and Ahn, W. S., "H-Infinity yaw moment control with brakes for improving driving performance and stability", *Proceedings of the 1999 IEEE/ASME International Conference on Advanced Intelligent Mechatronics*, AIM, September 19-23, 1999, Atlanta, GA, USA, pp 747-752.

[9] Drakunov, S.V., Ashrafi, B., and Rosiglioni, A., "Yaw Control Algorithm via Sliding Mode Control", *Proceedings of the American Control Conference*, v 1, Jun 28–30, 2000, Chicago, IL, USA, pp 580-583.

[10] Hac, A. and Bodie, M. O., "Improvements in vehicle handling though integrated control of chassis systems", *International Journal of Vehicle Design*, v 29, n 1-2, 2002, pp 23-50.

[11] Anwar, S., "A Parametric Model of an Eddy Current Electric Machine for Automotive Braking Applications", *IEEE Transactions on Control Systems Technology,* Vol. 12, Issue 3, May, 2004, pp. 422-427.

[12] Kiencke, U. and Nielsen, L., "Automotive Control System for Engine, Driveline, and Vehicle", *SAE International*, 2000.